An Analytical Model for Describing Tensile Behavior of FRCM

Yu Yuan and Gabriele Milani(✉)

Department of Architecture, Built Environment and Construction Engineering (ABC), Politecnico Di Milano, Piazza Leonardo da Vinci 32, 20133 Milan, Italy
gabriele.milani@polimi.it

Abstract. As a newly emerged strengthening material, FRCM (Fiber Reinforced Cementitious Matrix) has attracted the attention of many engineers and scholars due to the higher compatibility of the cementitious matrix with masonry structures compared to traditional organic matrix. Different from FRP (Fiber Reinforced Polymer) material that similarly can be externally applied onto the structures for strengthening, FRCM exhibits more complex failure modes due to the weaker performance of the matrix. To investigate the complex failure mechanism, the tensile test on FRCM coupon is a simple and intuitive method commonly used, in which the failure of both material and interface can be observed. In this article, an analytical model was proposed to reproduce the tensile behavior of FRCM, with the possibility to consider all the failure modes. A simplified mathematical model consisting of the components of the mortar layer, the fiber layer, and a zero-thickness interface gives the basis of force analysis, and from which the ODE system presenting the model behavior can be deduced and solved. This model was then validated against existing experimental results in terms of the global stress-strain relationships. It can be concluded that the proposed model is fast and stable, while able to reproduce the failure mode, global and local behavior of FRCM under tension.

Keywords: FRCM · Tensile test · Closed-form solution · Cracking

1 Introduction

For many existing masonry buildings, due to various damages caused by natural and human factors, as well as the poor seismic performance of the masonry structure itself, intervention and strengthening are often necessary. As a new strengthening strategy, the external application of composite materials to components can improve the load-bearing capacity and seismic performance of the structure without greatly increasing the weight of the structure and occupying space. Among them, FRCM (Fiber Reinforced Cement Matrix) has attracted attention in recent years in the area of masonry structure reinforcement. This is because, unlike the organic matrix used in FRP (Fiber Reinforced Polymer) strengthening systems, the inorganic matrix of FRCM ensures better compatibility with masonry materials, and facilitates the discharge of salt and moisture. For building heritages, an important advantage of FRCM is the reversibility of the interventions. An

R. Capozucca et al. (Eds.): ICSCES 2022, LNCE 317, pp. 244–252, 2023.
https://doi.org/10.1007/978-3-031-24041-6_20

important issue about the application of FRCM is the complex failure modes, not only failure will appear as the matrix-substrate debonding, but in the FRCM composite itself. That is, the mortar may crack, the fiber strip may slip inside the mortar, and even the fiber strip may break, due to the lower strength of the mortar matrix.

The tensile test is widely used as a simple and intuitive test [1–4], which can well characterize the various failure modes that FRCM may appear, although the test set-up and specimen preparation may have a large impact on the results. Therefore, in the case of limitations in comparing data from different experimental campaigns [2], the development of reasonable prediction models can be very meaningful, which can provide insights into explaining some experimental phenomena from a theoretical perspective. Numerical models have been developed specifically to describe the behavior of FRCMs under tension, such as modeling using finite element methods [4–6], or springs to characterize the interaction between materials [7]. In contrast, the model proposed in this paper has a faster calculation speed, and stable output due to the use of analytical solutions, while asking for only a few parameters.

To describe the FRCM coupon under classical tensile tests, a simplified mathematical model is established, including three parts, meaning the mortar layer, the fiber strip, and a zero-thickness interface. Three cases are separately considered to investigate the influence of failure for different components: 1) Case 1, which only considers the failure of mortar; 2) Case 2, which only considers the failure of the interface bond; 3) Case 3, in which both failures of mortar and interface will be considered. Then the situations where failures of both mortar and interface will appear can be discussed based on these two cases. The analytical approach is based on the closed-form solution of the ODE system derived from the equilibrium conditions of an infinitesimal part of the coupon, as well as the constitutive and geometric relationships. At different analysis moments and failures of components, different boundary conditions can be obtained to derive the closed-form solutions. This approach is then validated against existing experimental data for all cases considered. Good agreement can be found in terms of the global stress-strain relationship and bond strength. The occurrence of mortar cracking can also be presented by the model, however, due to the inhomogeneity of mortar mechanical properties and specimen geometry, manufacturing quality, etc., the location of cracks in the experiment cannot be exactly simulated.

2 The Analytical Model and Solutions

2.1 The Analytical Model

The analytical model is expected to describe the typical non-linear behavior of FRCM under tension. Based on the experimental phenomena, a simplified mathematical model was proposed, including three parts: (i) the mortar layer characterized by a perfectly elastic-brittle behavior; (ii) the fiber strip characterized by a fully elastic behavior throughout the analysis procedure; (iii) the zero-thickness interface characterized by a perfectly elastic-brittle shear stress-slip relationship which takes into consideration of the residual strength.

To assume that the material properties (mechanical and geometry) distributions along the width of the coupon are uniform, considering the symmetric loading conditions, we

can take only a quarter of the whole FRCM coupon for analysis at the beginning of the simulation as shown in Fig. 1 (a). Take an infinitesimal part of the FRCM for force analysis, according to the equilibrium condition we can write:

$$\begin{cases} t_f \frac{d\sigma_f}{dx} = \tau(s) \\ t_m \frac{d\sigma_m}{dx} = -\tau(s) \end{cases} \tag{1}$$

in which t_m is the thickness of the mortar layer, t_f is half of the thickness of the fiber strip. The tensile stress of mortar and fiber are denoted by σ_m and σ_f respectively. The shear stress along the mortar-fiber interface is denoted by $\tau(s)$, we assume an elastic-brittle behavior with a constant residual strength:

$$\begin{cases} \tau = K_i \cdot s \ (s \le \tau_m / K_i) \\ \tau = \tau_r \quad (s > \tau_m / K_i) \end{cases} \tag{2}$$

in which K_i is the initial elastic stiffness assumed for the interface, τ_m and τ_r are the maximum and residual shear strengths of the interface. And s is the difference of displacements between mortar (u_m) and fiber (u_f):

$$s = u_f - u_m \tag{3}$$

The constitutive laws of the materials at the elastic stage yield:

$$\begin{cases} \sigma_f = E_f \frac{du_f}{dx} \\ \sigma_m = E_m \frac{du_m}{dx} \end{cases} \tag{4}$$

in which E_m and E_f are Young's moduli of the mortar and fiber respectively. The ODE system can be obtained by combining Eq. (4) and Eq. (1).

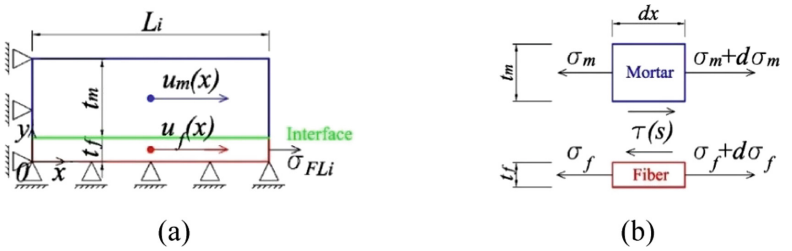

Fig. 1. The simplified mathematical model (a), and force analysis for the infinitesimals (b)

We will consider two moments to highlight in the global response the occurrence of unloading when crack generating:

1) Moment A, at which the tensile stress inside mortar reaches its maximum tensile strength;
2) Moment B, at which a crack appears at the same position mortar just gained its maximum strength, and the tensile stress at this position shifted to zero.

After the mortar cracks, we can take the uncracked mortar segment as a new object for analysis. And considering whether the model components enter the plastic stage, three cases might occur in each analyzed segment:

In Case 1, the interface behaves fully elastic until mortar cracking. Since it is assumed that the interface maintains elasticity before and after cracking, the same analytical method can be adopted for all the uncracked mortar segments under symmetrical conditions. At moment B, displacement translation will be performed to make the displacement of the new symmetric center (the center of the new uncracked segment) zero, thus making it possible to always take a quarter part of the segment for analysis.

In Case 2, the interface behaves fully plastic before mortar cracking. This situation may occur when the mortar length is too small, and the residual friction distributed along the interface is not able to provide enough energy to fracture the mortar. Thus, in Case 2, no further analysis will be performed, and the tensile procedure will be terminated when the fiber fractures. Two interface models with (Case 2-b) and without (Case 2-a) residual strength were considered in Case 2, to investigate the influence.

For Case 3, where both failures of mortar and interface will occur, the symmetric condition will no longer exist due to the interface entering partially before mortar cracking, and it is not possible for the failed interface to return elastic. The calculations will be more complex but still the same methodology to solve the ODE system. The simulation will be terminated when the fiber fractures, normally before this happens, Case 2 will appear for the mortar section without enough long length.

2.2 The Closed-Form Solutions

Case 1. In this case, we assume that the mortar matrix and the interface all behave as elastic before mortar cracks. We take the analysis for intact FRCM coupon as step $i = 1$; after the first crack appears in the middle, we denote the next analysis on the half segment as step $i = 2$, and so on. Combining Eq. (4) and Eq. (1), the following ODE system can be obtained:

$$\begin{bmatrix} \frac{du_f}{dx} \\ \frac{d\sigma_f}{dx} \\ \frac{du_m}{dx} \\ \frac{d\sigma_m}{dx} \end{bmatrix} = \begin{bmatrix} 0 & \frac{1}{E_f} & 0 & 0 \\ \frac{K_i}{t_f} & 0 & -\frac{K_i}{t_f} & 0 \\ 0 & 0 & 0 & \frac{1}{E_m} \\ -\frac{K_i}{t_m} & 0 & \frac{K_i}{t_m} & 0 \end{bmatrix} \begin{bmatrix} u_f \\ \sigma_f \\ u_m \\ \sigma_m \end{bmatrix} \tag{5}$$

The general solution of the ODE system can be obtained as below:

$$\begin{bmatrix} u_f \\ \sigma_f \\ u_m \\ \sigma_m \end{bmatrix} = C_1 \begin{bmatrix} 1 \\ 0 \\ 1 \\ 0 \end{bmatrix} + C_2 \left(\begin{bmatrix} 1 \\ 0 \\ 1 \\ 0 \end{bmatrix} x + \begin{bmatrix} 0 \\ E_f \\ 0 \\ E_m \end{bmatrix} \right) + C_3 \begin{bmatrix} -t_m\alpha \\ -t_m/t_f \\ t_m\beta \\ 1 \end{bmatrix} e^{\lambda_3 x} + C_4 \begin{bmatrix} t_m\alpha \\ -t_m/t_f \\ -t_m\beta \\ 1 \end{bmatrix} e^{\lambda_4 x} \tag{6}$$

in which:

$$\begin{cases} \lambda_3 = \sqrt{K_i(\frac{1}{E_m t_m} + \frac{1}{E_f t_f})} \\ \lambda_4 = -\sqrt{K_i(\frac{1}{E_m t_m} + \frac{1}{E_f t_f})} \\ \alpha = \sqrt{\frac{E_m t_m}{E_f t_f K_i (E_f t_f + E_m t_m)}} \\ \beta = \sqrt{\frac{E_f t_f}{E_m t_m K_i (E_f t_f + E_m t_m)}} \end{cases} \tag{7}$$

For determining the constants of integration, the boundary conditions of describing moment A are:

$$\begin{cases} u_f|_{x=0} = 0 \\ u_m|_{x=0} = 0 \\ \sigma_m|_{x=0} = f_{tm} \\ \sigma_m|_{x=L_i} = 0 \end{cases} \tag{8}$$

in which L_i is the length of the quarter of the coupon under analysis, and we have $L_i = L/2^i$ for step i.

After displacement translation, for moment B we can write the following boundary conditions:

$$\begin{cases} u_f|_{x=0} = -u_{fLi}^{iA} \\ u_f|_{x=L_i} = 0.5 u_{fLi}^{iA} \\ \sigma_m|_{x=0} = 0 \\ \sigma_m|_{x=L_i} = 0 \end{cases} \tag{9}$$

in which u_{fLi}^{iA} is the fiber displacement at the loading edge solved in moment i-A.

Case 2. In this case, we assume that the mortar will not break, while the interface will enter the plastic stage before the fiber fractures. Assume the local abscissa of the point at which the interface transforms from elastic to plastic stage is x_r, which will be assigned gradually from L_i to 0, to simulate the procedure of increasing interface slip until the fiber fractures.

For the elastic range ($0 \le x \le x_r$), the ODE system is the same as Eq. (5), which can be solved with different boundary conditions:

$$\begin{cases} u_f|_{x=0} = 0 \\ u_m|_{x=0} = 0 \\ (u_f - u_m)|_{x=x_r} = s_e \\ \sigma_m|_{x=x_r} = \frac{\tau_r(L_i - x_r)}{t_m} \end{cases} \tag{10}$$

For the plastic range ($x_r < x \le L_i$), the displacements of fiber and mortar at a certain point along the plastic range are:

$$u_f = u_f|_{x=x_r} + \int_{x_r}^{x} \frac{\sigma_f}{E_f} dx \tag{11}$$

in which σ_f is the tensile stress of fiber at x. The equilibrium condition of the plastic section gives:

$$\sigma_f = \sigma_f|_{x=x_r} + \frac{\tau_r(x - x_r)}{t_f} \tag{12}$$

Combining the constitutive laws of mortar and fiber, the integration of Eq. (11) gives the solutions along the plastic range:

$$\begin{cases} u_f = \frac{f_{tf}}{E_f} x + \frac{\tau_r}{E_f t_f}(\frac{1}{2}x^2 - L_i x) \\ \sigma_f = f_{tf} - \frac{\tau_r(L_i - x)}{t_f} \\ u_m = \frac{\tau_r}{E_m t_m}(L_i x - \frac{1}{2}x^2) \\ \sigma_m = \frac{\tau_r(L_i - x)}{t_m} \end{cases} \tag{15}$$

3 Validation

In this section, the experimental results of the FRCM coupon under the tensile test provided by Bertolesi et al. [4] were adopted to verify the reliability of the developed analytical model. In this experimental campaign carried out at the Polytechnic University of Milan, the FRCM coupon cast by cementitious mortar on the PBO fiber grid was tested, as well as the geometrical and mechanical properties of both two components, giving the possibilities to assume the parameters for validation as listed in Table 1.

It is now generally accepted that the constitutive behavior of FRCM composites in tension can be idealized as a trilinear relationship [5, 8]. In the first stage, the material is not cracked and the stiffness of the composite should ideally be the stiffness of the mortar. In the second stage, multiple cracks began to form, and the load-displacement (or stress-strain) curve oscillated multiple times. In the third stage, the cracks will propagate until the fibers fracture, the mortar layer has almost failed and the composite should ideally

Table 1. Parameters adopted to validate the present model.

Em [MPa]	t_m [mm]	f_{tm} [MPa]	E_F [MPa]	f_{tf} [MPa]	t_F [mm]	B_F [mm]	L [mm]	τ_m [N/mm^2]	K [N/mm^3]	τ_r [N/mm^2]
6000	5	3.65	215900	3397	0.035	40	280	2.5	166.67	0.35

reproduce the elastic modulus of the dry fibers. The results in terms of the global coupon stress-strain curves obtained by the present model and experimental data are compared in Fig. 2. It can be concluded that the results generated by the present model are in good agreement with the experimental results in terms of trend and range, fitting into the generally recognized three-stages constitutive model. Similar ultimate strength and strain can be gained, as well as the beginning of the second stage, which should ideally be the moment mortar reaches its tensile strength.

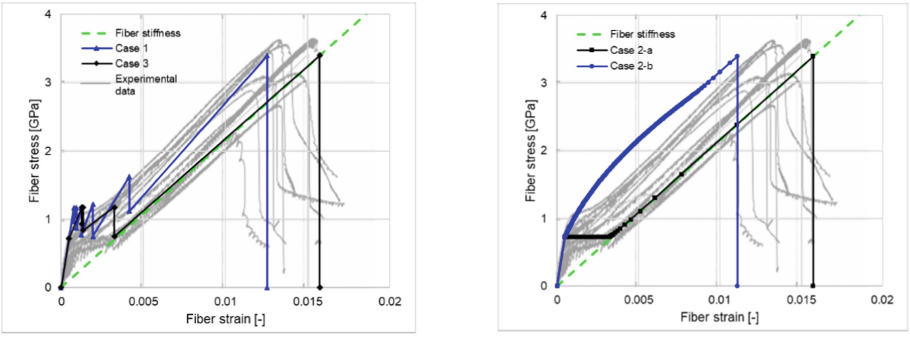

(a) (b)

Fig. 2. The stress-strain relationships until fiber fracture for Cases 1 and 3 (a), and Case 2 (b) gained via the present model and experimental tests

The proposed analytical method can also provide the local behavior of FRCM under tension, including stress and displacement distributions of fibers and mortar along the length of the specimen. Due to the limitation of the length of the article, here only gives an example of the tensile stress distribution of the mortar until the specimen fails (the fibers fracture), as shown in Fig. 3. For Cases 1 and 3, the solid line represents the mortar stress at moment A (the mortar reaches its maximum tensile strength), while the dashed line represents moment B (the mortar breaks). While For case 2, the graphs in Fig. 3-c and Fig. 3-d show the distribution of mortar tensile stress with the increase of external force, the difference lies in the residual friction along the interface after interface failure. For Case 1 in Fig. 3-a, a clear symmetry pattern can be identified, thanks to the assumption of material and geometry symmetries, and the calculation process of constantly changing the symmetric center. For Case 3, the distribution of mortar stress is no longer symmetrical regarding the cracks, due to interface debonding that occurs first at the loading edge.

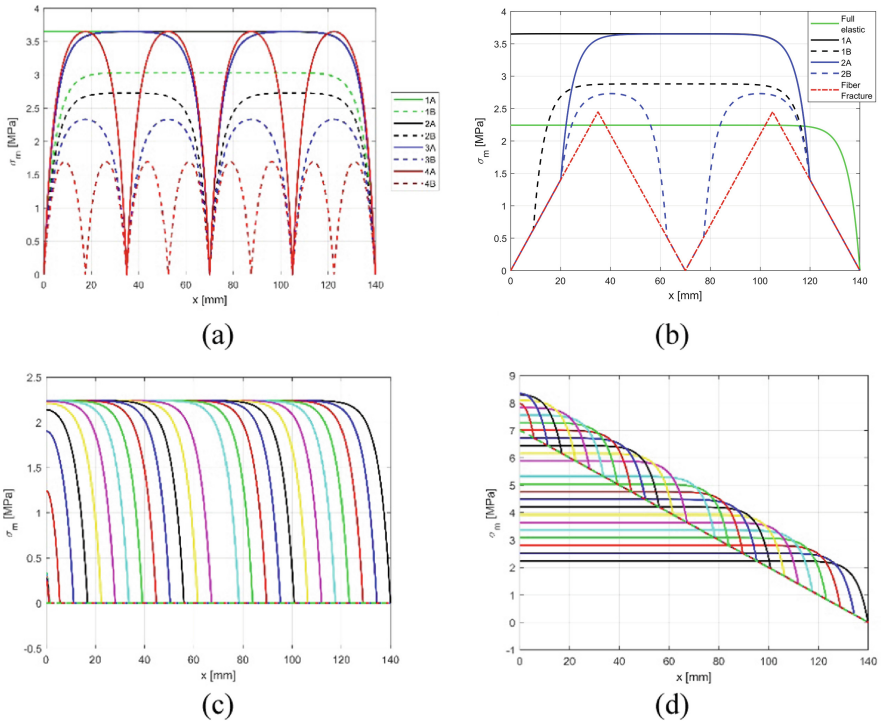

Fig. 3. Distribution of mortar tensile stress until fiber fracture for Case1 (a), Case 3 (b), Case 2-a (c), and Case 2-b (d)

4 Conclusions

This study presents an analytical model which can consider all the failure modes of the FRCM coupon under tension. A classical mathematical model which consists of the mortar and fiber layers and zero-thickness interfaces was considered. A multi-segment linear relationship was chosen to describe the interface relationship, allowing us to gain the solutions analytically. This method can satisfactorily reproduce the tensile behavior of the FRCM coupon with little calculation effort and few parameters. The obtained results are in good agreement with the experimental results in terms of range and trend, fitting into the generally accepted trilinear constitutive law. Moreover, the local behavior of the entire system can be determined, as well as the locations of mortar cracking. But except for the one crack appearing at the center of the specimen, the locations of mortar cracking in the actual specimen is rather random due to internal flaws or eccentric loading.

Acknowledgments. Yu Yuan would like to acknowledge the financial support provided by the Chinese Scholarship Council (CSC) for performing her Ph.D. program at the Technical University of Milan, Italy.

References

1. de Felice, G., et al.: Mortar-based systems for externally bonded strengthening of masonry. Mater. Struct. **47**(12), 2021–2037 (2014). https://doi.org/10.1617/s11527-014-0360-1
2. D'antino, T., Papanicolaou, C.C.: Comparison between different tensile test set-ups for the mechanical characterization of inorganic-matrix composites. Constr. Build. Mater. **171**, 140–151 (2018). https://doi.org/10.1016/j.conbuildmat.2018.03.041
3. Arboleda, D., Carozzi, F.G., Nanni, A., Poggi, C.: Testing procedures for the uniaxial tensile characterization of fabric reinforced cementitious matrix (FRCM) composites. J. Compos. Constr **20**, 04015063 (2016). https://doi.org/10.1061/(ASCE)CC.1943-5614.0000626
4. Carozzi, F.G., Poggi, C.: Mechanical properties and debonding strength of Fabric Reinforced Cementitious Matrix (FRCM) systems for masonry strengthening. Compos. B Eng. **70**, 215–230 (2015). https://doi.org/10.1016/j.compositesb.2014.10.056
5. Bertolesi, E., Carozzi, F.G., Milani, G., Poggi, C.: Numerical modeling of Fabric Reinforce Cementitious Matrix composites (FRCM) in tension. Constr. Build. Mater. **70**, 531–548 (2014). https://doi.org/10.1016/j.conbuildmat.2014.08.006
6. Nerilli, F., Marfia, S., Sacco, E.: Micromechanical modeling of the constitutive response of FRCM composites. Constr. Build. Mater. **236**, 117539 (2020). https://doi.org/10.1016/j.conbuildmat.2019.117539
7. Grande, E., Milani, G.: Numerical simulation of the tensile behavior of FRCM strengthening systems. Compos. B Eng. **189**, 107886 (2020). https://doi.org/10.1016/j.compositesb.2020.107886
8. Hartig, J., Jesse, F., Schicktanz, K., Häußler-Combe, U.: Influence of experimental setups on the apparent uniaxial tensile load-bearing capacity of textile reinforced concrete specimens. Mater. Struct. **45**(3), 433–446 (2012). https://doi.org/10.1617/s11527-011-9775-0